Supplemental materials for

# Modeling of eicosanoid fluxes in macrophages reveals functional coupling between cyclooxygenases and terminal synthases

Yasuyuki Kihara[#], Shakti Gupta[#], Mano R. Maurya, Aaron Armando, Ishita Shah, Oswald Quehenberger, Christopher K. Glass, Edward A. Dennis[*], and Shankar Subramaniam[*].

*To whom correspondence should be addressed.
e-mail: shankar@ucsd.edu, edennis@ucsd.edu
# equal contribution

## MATERIALS AND METHODS

***Outlier detection.*** For kinetic modeling purposes, outlier data values for lipids were detected at each time-point by a z-test, in which, for a chosen time point, we exclude one data value out of the three from the computation of mean and standard deviation, and then test the z-score of the excluded data value with a two-tailed ~95% confidence ($|z| > 2.0$) test. This process was repeated for each replicate. With this strategy, the outlier does not affect the z-test during the outlier detection process. Since there are only 3 biological replicates, at most one data value is removed. The resulting data from all the replicates were averaged at each time-point.

***Parameter estimation.*** Through the minimization of the objective function of Eq. 3, the initial concentrations of the metabolites were also optimized in a narrow range around the experimental values. Different weights can be assigned to the fit error to improve the fit. For this study, $w_1$ was set to 1 in both pathways and $w_2$ was set to 0 and 0.1 for COX and LOX pathways, respectively. Further, the data were measured at irregular time intervals (longer intervals at later times). This led to relatively poor fit at later time points. To resolve this issue, the point-wise error was scaled by n-th root of the length of the time interval ($n$ = 10 and 100 for COX and LOX pathways, respectively).

***Estimation of uncertainty in the calculated parameters.*** The effect of biological variation of lipidomic and transcriptomic measurements in the calculated parameters was accounted through parameter uncertainty analysis. First, the standard error of the mean (SEM) in the lipid and the gene data at each time point was calculated. A candidate dataset for parameter estimation was created by generating the $nsp \times nt$ random matrix utilizing the normal distribution. Then it was scaled with the corresponding SEM and the scaled value matrix was added to the mean-value data on lipids and genes to generate a candidate date set. The parameters were estimated using the candidate dataset to produce one parameter-value set. Next, the parameter estimation was repeated $k$ times to generate $k$ parameter-value sets ($k$ = 20 in our simulation). Finally, the SEM for each parameter across the $k$ sets was computed.

***Timescale analysis.*** First, the steady-state was identified by simulating the system corresponding to the control condition (no stimulus) for a long time ($t$ =1000 h). The Jacobian was computed through numerical differentiation of the expressions on the right-hand sides of the ODEs with respect to the state variables. Then, the eigenvalues and eigenvectors of the Jacobian matrix of ordinary differential equations at steady-state conditions were calculated. For each eigenvalue, the metabolites with substantial contribution to the corresponding eigenvector were identified. When a metabolite contributed significantly in two or more eigenvectors spanning two different eigenvalue ranges, it was assigned to the smaller eigenvalue range, because the fast time manifold only determines its initial transients and the slow manifold governs the later response leading to steady state.

***Statistical analysis.*** Experimental results were expressed as mean ± SEM. For COX inhibitor experiments, data were

analyzed statistically by Kruskal-Wallis test followed by Dunn's multiple comparison test using Prism (GraphPad Software, Inc.). p-values < 0.05 were considered to be statistically significant. To test the goodness of the fits, we have compared the variance for the fit to the variance in the experimental (replicate) data (Treatment and Control data combined) using F-test as follows:

$$F = \frac{SSE_{fit}/(2\times nt)}{SSE_{\exp}/(2\times nt\times(nr-1))} = \frac{\left(\sum_{j=1}^{nt}(Y_j^{Trt}-\overline{X}_j^{Trt})^2+\sum_{j=1}^{nt}(Y_j^{Ctrl}-\overline{X}_j^{Ctrl})^2\right)/(2\times nt)}{\left(\sum_{j=1}^{nt}\left[\sum_{i=1}^{nr}(X_{ij}^{Trt}-\overline{X}_j^{Trt})^2/(nr-1)\right]+\sum_{j=1}^{nt}\left[\sum_{i=1}^{nr}(X_{ij}^{Ctrl}-\overline{X}_j^{Ctrl})^2/(nr-1)\right]\right)/(2\times nt)}$$

,

where $X$, $\overline{X}$ and $Y$ denote the experimental data, mean experimental data and simulated (fitted) data at time point $j$, respectively, $nt$ is the number of time-points ($nt$ = 8), $nr$ is the number of replicates ($nr$ = 3, indexed as $i$), and Trt and Ctrl are treatment and control groups, respectively.

***ODEs used in the single $PGH_2$ model.*** The differential equations describing the rate of change of metabolite concentrations are as follows.

<u>COX pathway:</u>

$$\frac{d[PGH_2]}{dt} = (k_{C1}[Ptgs1]+k_{C2}[Ptgs2])[AA]-(k_{C4}+k_{C5}[Tbxas1]+k_{C7}+k_{C9}[Ptges]+k_{C11}[Ptgds])[PGH_2]$$

$$\frac{d[TXB_2]}{dt} = k_{C5}[Tbxas1][PGH_2]-k_{C6}[TXB_2]$$

$$\frac{d[PGF_{2a}]}{dt} = k_{C7}[PGH_2]-k_{C8}[PGF_{2a}]$$

$$\frac{d[PGE_2]}{dt} = k_{C9}[Ptges][PGH_2]-k_{C10}[PGE_2]$$

$$\frac{d[PGD_2]}{dt} = k_{C11}[Ptgds2][PGH_2]-(k_{C12}+k_{C13}[Hpgd]+k_{C17}+k_{C19})[PGD_2]$$

$$\frac{d[15k\text{-}PGD_2]}{dt} = k_{C13}[Hpgd])[PGD_2]-(k_{C14}+k_{C15}[Ltb4dh])[15k\text{-}PGD_2]$$

$$\frac{d[DHKPGD_2]}{dt} = k_{C15}[Ltb4dh][15k\text{-}PGD_2]-k_{C16}[DHKPGD_2]$$

$$\frac{d[15d\text{-}PGD_2]}{dt} = k_{C17}[PGD_2]-k_{C18}[15d\text{-}PGD_2]$$

$$\frac{d[PGJ_2]}{dt} = k_{C19}[PGD_2]-(k_{C20}+k_{C21})[PGJ_2]$$

$$\frac{d[15d\text{-}PGJ_2]}{dt} = k_{C21}[PGJ_2]-k_{C22}[15d\text{-}PGJ_2]$$

<u>LOX pathway:</u>

$$\frac{\mathrm{d}[5\text{-HETE}]}{\mathrm{dt}} = k_{L1}[Alox5][\mathrm{AA}] - k_{L3}[5\text{-HETE}]$$

$$\frac{\mathrm{d}[\mathrm{LTA}_4]}{\mathrm{dt}} = k_{L2}[Alox5][\mathrm{AA}] - (k_{L5} + k_{L6} + k_{L9}[Lta4h] + k_{L10})[\mathrm{TXB}_2]$$

$$\frac{\mathrm{d}[\mathrm{LTB}_4]}{\mathrm{dt}} = k_{L6}[Lta4h][\mathrm{LTA}_4] - (k_{L7}[Ltb4dh] + k_{L8})[\mathrm{LTB}_4]$$

$$\frac{\mathrm{d}[12\text{-epi-LTB}_4]}{\mathrm{dt}} = k_{L9}[\mathrm{LTA}_4] - k_{L11}[12\text{-epi-LTB}_4]$$

$$\frac{\mathrm{d}[6\text{-trans-12-epi-LTB}_4]}{\mathrm{dt}} = k_{L10}[\mathrm{LTA}_4] - k_{L12}[6\text{-trans-12-epi-LTB}_4]$$

$$\frac{\mathrm{d}[15\text{-HETE}]}{\mathrm{dt}} = k_{L13}[Alox15][\mathrm{AA}] - k_{L14}[15\text{-HETE}]$$

***ODEs used in the $PGH_2$-divided model.*** The differential equations describing the rate of change of metabolite concentrations in the COX pathway are as follows:

$$\frac{\mathrm{d}[\mathrm{C1PGH}_2]}{\mathrm{dt}} = k_{CP1}[Ptgs1][\mathrm{AA}] - (k_{CP4} + k_{CP6}[Tbxas1] + k_{C9} + k_{CP12}[Ptges] + k_{CP15}[Ptgds])[\mathrm{PGH}_2]$$

$$\frac{\mathrm{d}[\mathrm{C2PGH}_2]}{\mathrm{dt}} = k_{CP2}[Ptgs2][\mathrm{AA}] - (k_{CP5} + k_{CP7}[Tbxas1] + k_{C10} + k_{CP13}[Ptges] + k_{CP16}[Ptgds])[\mathrm{PGH}_2]$$

$$\frac{\mathrm{d}[\mathrm{TXB}_2]}{\mathrm{dt}} = (k_{CP6}[\mathrm{C1PGH}_2] + k_{CP7}[\mathrm{C2PGH}_2])[Tbxas1] - k_{CP8}[\mathrm{TXB}_2]$$

$$\frac{\mathrm{d}[\mathrm{PGF}_{2a}]}{\mathrm{dt}} = k_{CP9}[\mathrm{C1PGH}_2] + k_{CP10}[\mathrm{C1PGH}_2] - k_{CP11}[\mathrm{PGF}_{2a}]$$

$$\frac{\mathrm{d}[\mathrm{PGE}_2]}{\mathrm{dt}} = (k_{CP12}[\mathrm{C1PGH}_2] + k_{CP13}[\mathrm{C2PGH}_2])[Ptges] - k_{CP14}[\mathrm{PGE}_2]$$

$$\frac{\mathrm{d}[\mathrm{PGD}_2]}{\mathrm{dt}} = (k_{CP15}[\mathrm{C1PGH}_2] + k_{CP16}[\mathrm{C2PGH}_2])[Ptgds2] - (k_{CP17} + k_{CP18}[Ltb4dh] + k_{C22} + k_{CP24})[\mathrm{PGD}_2]$$

$$\frac{\mathrm{d}[15\text{k-PGD}_2]}{\mathrm{dt}} = k_{CP18}[Hpgd][\mathrm{PGD}_2] - (k_{CP19}[Ltb4dh] + k_{CP20})[15\text{k-PGD}_2]$$

$$\frac{\mathrm{d}[\mathrm{DHKPGD}_2]}{\mathrm{dt}} = k_{CP20}[Ltb4dh][15\text{k-PGD}_2] - k_{CP21}[\mathrm{DHKPGD}_2]$$

$$\frac{\mathrm{d}[15\text{d-PGD}_2]}{\mathrm{dt}} = k_{CP22}[\mathrm{PGD}_2] - k_{CP23}[15\text{d-PGD}_2]$$

$$\frac{\mathrm{d}[\mathrm{PGJ}_2]}{\mathrm{dt}} = k_{CP24}[\mathrm{PGD}_2] - (k_{CP25} + k_{CP26})[\mathrm{PGJ}_2]$$

$$\frac{\mathrm{d}[15\text{d-PGJ}_2]}{\mathrm{dt}} = k_{CP26}[\mathrm{PGJ}_2] - k_{CP27}[15\text{d-PGJ}_2]$$

**SUPPLEMENTAL TABLE**

**Table S1: Chemical reactions, rate equations and calculated kinetic parameters for the COX pathway**

| Reactions | Rate equations | Parameters |
|---|---|---|
| [*Ptgs1*] AA → $PGH_2$ | $v_{C1} = k_{C1}$[*Ptgs1*][AA] | $k_{C1}$ = 0.0198 ± 0.0038 |
| [*Ptgs2*] AA → $PGH_2$ | $v_{C2} = k_{C2}$[*Ptgs2*][AA] | $k_{C2}$ = 0.0010 ± 0.0001 |
| AA → | $v_{C3} = k_{C3}$[AA] | $k_{C3} = 10^{-15}$ |
| $PGH_2$ → | $v_{C4} = k_{C4}[PGH_2]$ | $k_{C4}$ = 3.2301 ± 0.0380 |
| [*Tbxas1*] $PGH_2$ → $TXB_2$ | $v_{C5} = k_{C5}$[*Tbxas1*] $[PGH_2]$ | $k_{C5}$ = 0.0022 ± 0.0016 |
| $TXB_2$ → | $v_{C6} = k_{C6}[TXB_2]$ | $k_{C6}$ = 0.0108 ± 0.0134 |
| $PGH_2$ → $PGF_2\alpha$ | $v_{C7} = k_{C7}[PGH_2]$ | $k_{C7}$ = 0.0004 ± 0.0004 |
| $PGF_2\alpha$ → | $v_{C8} = k_{C8}[PGF_2\alpha]$ | $k_{C8}$ = 0 ± 0.0396 |
| [*Ptges*] $PGH_2$ → $PGE_2$ | $v_{C9} = k_{C9}$[*Ptges*]$[PGH_2]$ | $k_{C9}$ = 0.0019 ± 0.0003 |
| $PGE_2$ → | $v_{C10} = k_{C10}[PGE_2]$ | $k_{C10}$ = 3.3030 ±0.0500 |
| [*Ptgds2*] $PGH_2$ → $PGD_2$ | $v_{C11} = k_{C11}$[*Ptgds2*]$[PGH_2]$ | $k_{C11}$= 0.5801 ± 0.0633 |
| $PGD_2$ → | $v_{C12} = k_{C12}[PGD_2]$ | $k_{C12}$ = 0.5230 ± 0.0745 |
| [*Hpgd*] $PGD_2$ → 15k-$PGD_2$ | $v_{C13} = k_{C13}$[*Hpgd*]$[PGD_2]$ | $k_{C13}$ = 0.0044 ± 0.0019 |
| 15k-$PGD_2$ → | $v_{C14} = k_{C14}$[15k-$PGD_2$] | $k_{C14}$ = 0.5227 ± 0.0340 |
| [*Ltb4dh*]15k-$PGD_2$ → DHK-$PGD_2$ | $v_{C15} = k_{C15}$[*Ltb4dh*][15k-$PGD_2$] | $k_{C15}$ = 0.1676 ± 0.0383 |
| DHK-$PGD_2$ → | $v_{C16} = k_{C16}$[DHK-$PGD_2$] | $k_{C16}$ = 0.0315 ± 0.0131 |
| $PGD_2$ → 15d-$PGD_2$ | $v_{C17} = k_{C17}[PGD_2]$ | $k_{C17}$ = 0.0364 ± 0.0316 |
| 15d-$PGD_2$ → | $v_{C18} = k_{C18}$[15d-$PGD_2$] | $k_{C18}$ = 0.0029 ± 0.0229 |
| $PGD_2$ → $PGJ_2$ | $v_{C19} = k_{C19}[PGD_2]$ | $k_{C19}$ = 0.0260 ± 0.0059 |
| $PGJ_2$ → | $v_{C20} = k_{C20}[PGJ_2]$ | $k_{C20}$ = 0 ± 0.0467 |
| $PGJ_2$ → 15d-$PGJ_2$ | $v_{C21} = k_{C21}[PGJ_2]$ | $k_{C21}$ = 0.1508 ± 0.0231 |
| 15d-$PGJ_2$ → | $v_{C22} = k_{C22}$[15d-$PGJ_2$] | $k_{C22}$ = 0.6159 ± 0.0617 |

The unit of the parameters in first-order reactions is 1/hr. The unit of parameters in second-order reactions is also 1/hr because it involves gene/protein as a modifier as we have used fold change data with respect to controls for these variables. The parameters are described as calculated parameter ± standard-error of mean (SEM) calculated from uncertainty analysis.

**Table S2: Chemical reactions, rate equations and calculated kinetic parameters for LOX pathways**

| Reactions | Rate equations | Parameters |
|---|---|---|
| [*Alox5*] AA → 5-HETE | $v_{L1} = k_{L1}$[*Alox5*][AA] | $k_{L1}$ = 0.0011 ± 0.00009 |
| [*Alox5*] AA → $LTA_4$ | $v_{L2} = k_{L2}$[*Alox5*][AA] | $k_{L2}$ = 0.0006 ± 0.00002 |
| 5-HETE → | $v_{L3} = k_{L3}$[5-HETE] | $k_{L3}$ = 2.6877 ± 0.1900 |
| AA → | $v_{L4} = k_{L4}$[AA] | $k_{L4} = 10^{-15}$ |
| $LTA_4$ → | $v_{L5} = k_{L5}[LTA_4]$ | $k_{L5}$ = 0.7671 ± 0.0838 |
| [*Lta4h*] $LTA_4$ → $LTB_4$ | $v_{L6} = k_{L6}$[*Lta4h*][$LTA_4$] | $k_{L6}$ = 1.0354 ± 0.0434 |
| [*Ltb4dh*] $LTB_4$ → | $v_{L7} = k_{L7}$[*Ltb4dh*] [$LTB_4$] | $k_{L7}$ = 1.2865 ± 0.0729 |
| $LTB_4$ → | $v_{L8} = k_{L8}[LTB_4]$ | $k_{L8}$ = 1.0775 ± 0.1109 |
| $LTA_4$ → 12-*epi*-$LTB_4$ | $v_{L9} = k_{L9}[LTA_4]$ | $k_{L9}$ = 1.7269 ± 0.0330 |
| $LTA_4$ → 6-*trans*-12-*epi*-$LTB_4$ | $v_{L10} = k_{L10}[LTA_4]$ | $k_{L10}$ = 1.0428 ± 0.0560 |
| 12-*epi*-$LTB_4$ → | $v_{L11} = k_{L11}$[12-*epi*-$LTB_4$] | $k_{L11}$ = 2.9604 ± 0.1023 |
| 6-*trans*-12-*epi*-$LTB_4$ → | $v_{L12} = k_{L12}$[6-*trans*-12-*epi*-$LTB_4$] | $k_{L12}$ = 2.2678 ± 0.0962 |
| [*Alox15*] AA → 15-HETE | $v_{L13} = k_{L13}$[*Alox15*][AA] | $k_{L13}$ = 0.0001 ± 0.00003 |
| 15-HETE → | $v_{L14} = k_{L14}$[15-HETE] | $k_{L14}$ = 0.2466 ± 0.1262 |

The unit of the parameters in first-order reactions is 1/hr. The unit of parameters in second-order reactions is also 1/hr because it involves gene/protein as a modifier as we have used fold change data with respect to controls for these variables. The parameters are described as calculated parameter ± SEM calculated from uncertainty analysis.

**Table S3:** The results of F test for Figs. 2, 3, S4 and S5.

| | **Single $PGH_2$ model** | | **$PGH_2$ -divided model** | |
|---|---|---|---|---|
| Metabolites | Fig. 2 (dataset A) | Fig. 3 (dataset B) | Fig. S4 (dataset A) | Fig. S5 (dataset B) |
| $PGD_2$ | 0.3205 | 0.3054 | 0.4687 | 0.5102 |
| $PGE_2$ | 0.1934 | 0.2289 | 0.1654 | 0.1664 |
| $TXB_2$ | 0.0518 | 0.0247 | 0.0083 | 0.0067 |
| $PGF_{2\alpha}$ | 0.0172 | 0.0279 | 0.0046 | 0.0090 |
| 15d-$PGD_2$ | 0.0282 | 0.2078 | 0.0290 | 0.0365 |
| DHK-$PGD_2$ | 0.1015 | 0.2903 | 0.0770 | 0.4562 |
| $PGJ_2$ | 0.0025 | 0.0115 | 0.0143 | 0.0161 |
| 15d-$PGJ_2$ | 0.0303 | 0.0793 | 0.0222 | 0.0555 |
| $LTB_4$ | 0.1213 | 0.1098 | N.D. | N.D. |
| 12-epi-$LTB_4$ | 0.0791 | 0.0808 | N.D. | N.D. |
| 6t-12e-$LTB_4$ | 0.0587 | 0.0572 | N.D. | N.D. |
| 5-HETE | 0.2997 | 0.2051 | N.D. | N.D. |
| 15-HETE | 0.0979 | 0.0672 | N.D. | N.D. |

F values were calculated as described in Materials and Methods. F values smaller than $F_{0.05}(16,32) = 0.4580$ (except for $PGD_2$) indicates that fit-error is statistically smaller than the experimental error. For $PGD_2$, F is smaller than $F_{0.95}(16,32) = 1.97$, indicating statistically equal variance in simulated (fitted) and experimental data. N.D.: not determined.

**Table S4:** Chemical reactions and calculated kinetic parameters in $PGH_2$-divided model.

| Reactions | Parameters (Non-primed) | Parameters (KLA-primed) |
|---|---|---|
| [*Ptgs1*] AA → $C1PGH_2$ | $k_{CP1}$ = 0.0163 ± 0.0009 | $k_{CP'1}$ = 0.0154 |
| [*Ptgs2*] AA → $C2PGH_2$ | $k_{CP2}$ = 0.0005 ± 0.00004 | $k_{CP'2}$ = 0.0004 |
| AA → | $k_{CP3}$ = $10^{-15}$ | $k_{CP'3}$ = $10^{-15}$ |
| $C1PGH_2$ → | $k_{CP4}$ = 0.9126 ± 0.0281 | $k_{CP'4}$ = 0.9406 |
| $C2PGH_2$ → | $k_{CP5}$ = 1.4606 ± 0.0217 | $k_{CP'5}$ = 1.4823 |
| [*Tbxas1*] $C1PGH_2$ → $TXB_2$ | $k_{CP6}$ = 0.0047 ±0.0024 | $k_{CP'6}$ = 0.0039 |
| [*Tbxas1*] $C2PGH_2$ → $TXB_2$ | $k_{CP7}$ = 0 ± 0.0002 | $k_{CP'7}$ = 0.0002 |
| $TXB_2$ → | $k_{CP8}$ = 0.0138 ± 0.0132 | $k_{CP'8}$ = 0.0074 |
| $C1PGH_2$ → $PGF_2\alpha$ | $k_{CP9}$ = 0.0018 ± 0.0007 | $k_{CP'9}$ = 0.0011 |
| $C2PGH_2$ → $PGF_2\alpha$ | $k_{CP10}$ = 0 ± 0.00008 | $k_{CP'10}$ = 0.0001 |
| $PGF_2\alpha$ → | $k_{CP11}$= 0.0500 ± 0.0412 | $k_{CP'11}$ = 0.0088 |
| [*Ptges*] $C1PGH_2$ → $PGE_2$ | $k_{CP12}$ = 0.0002 ± 0.0002 | $k_{CP'12}$ = 0 |
| [*Ptges*] $C2PGH_2$ → $PGE_2$ | $k_{CP13}$ = 0.0026 ± 0.0002 | $k_{CP'13}$ = 0.0024 |
| $PGE_2$ → | $k_{CP14}$ = 3.5289 ± 0.0191 | $k_{CP'14}$ = 3.5480 |
| [*Ptgds2*] $C1PGH_2$ → $PGD_2$ | $k_{CP15}$ = 0.2806 ± 0.0390 | $k_{CP'15}$ = 0.2416 |
| [*Ptgds2*] $C2PGH_2$ → $PGD_2$ | $k_{CP16}$ = 0.1970 ± 0.0354 | $k_{CP'16}$ = 0.2015 |
| $PGD_2$ → | $k_{CP17}$ = 0.2850 ± 0.0377 | $k_{CP'17}$ = 0.3227 |
| [*Ltb4dh*] $PGD_2$ → 15k-$PGD_2$ | $k_{CP18}$ = 0.0053 ± 0.0084 | $k_{CP'18}$ = 0.0014 |
| 15k-$PGD_2$ → | $k_{CP19}$ = $10^{-5}$ ± 0.0140 | $k_{CP'19}$ = 0.0140 |
| [*Ptgr*]15k-$PGD_2$ → DHK-$PGD_2$ | $k_{CP20}$ = 0.3811 ± 0.0530 | $k_{CP'20}$ = 0.4341 |
| DHK-$PGD_2$ → | $k_{CP21}$ = 0.0899 ± 0.0660 | $k_{CP'21}$ = 0.0298 |
| $PGD_2$ → 15d-$PGD_2$ | $k_{CP22}$ = 0.0807 ± 0.0221 | $k_{CP'22}$ = 0.0874 |
| 15d-$PGD_2$ → | $k_{CP23}$ = 0.0502 ± 0.0300 | $k_{CP'23}$ = 0.0802 |
| $PGD_2$ → $PGJ_2$ | $k_{CP24}$ = 0.0292 ± 0.0125 | $k_{CP'24}$ = 0.0241 |
| $PGJ_2$ → | $k_{CP25}$ = 0.0033 ± 0.1180 | $k_{CP'25}$ = 0 |
| $PGJ_2$ → 15d-$PGJ_2$ | $k_{CP26}$ = 0.1043 ± 0.0264 | $k_{CP'26}$ = 0.0786 |
| 15d-$PGJ_2$ → | $k_{CP27}$ = 0.3846 ± 0.0555 | $k_{CP'27}$ = 0.3292 |

The unit of the parameters in first-order reactions is 1/hr. The unit of parameters in second-order reactions is also 1/hr because it involves gene/protein as a modifier as we have used fold change data with respect to controls for these variables. The parameters are described as calculated parameter ± SEM calculated from uncertainty analysis.

**SUPPLEMENTAL FIGURES**

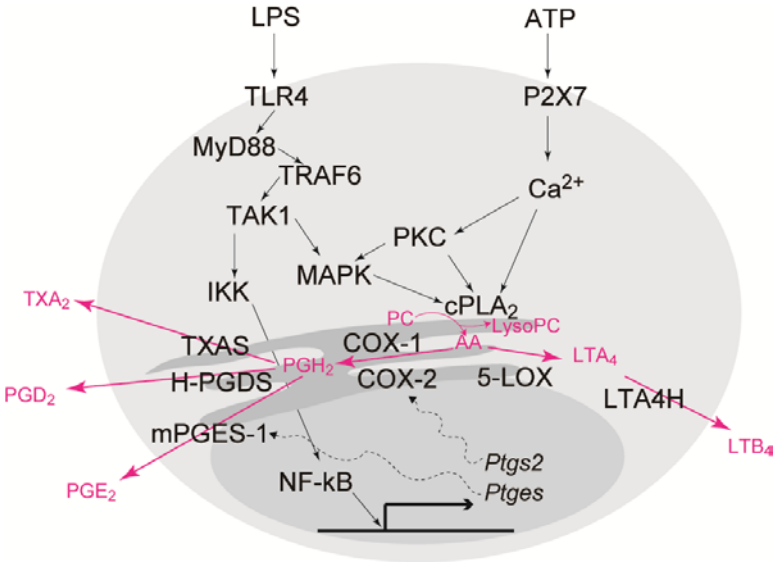


**Fig. S1 Intracellular signaling and eicosanoid metabolic network in macrophages.** LPS-TLR4 signaling activates MAP kinase (MAPK) and NF-κB pathways. COX-2 and mPGES-1 gene expression is induced through NF-κB. ATP increases intracellular $Ca^{2+}$ through $P_2X_7$ receptor, resulting in $cPLA_2$ translocation from cytosol to ER membrane and liberate AA from phosphatidylcholine (PC). MAPK and protein kinase C (PKC) phosphorylate $cPLA_2$ to promote its enzymatic activity.

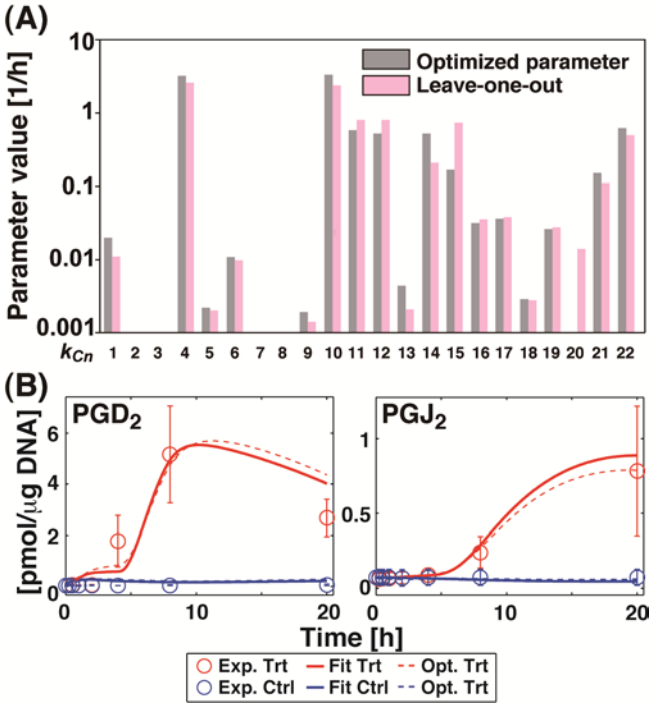


**Fig. S2 Validation of the computational model.** (A) The parameters by leave-one-metabolite-out methods are compared with calculated parameters. (B) The simulation results of $PGD_2$ and $PGJ_2$ are shown as red and blue curves for Trt and Ctrl. The dotted lines are simulation results obtained in Fig. 2.

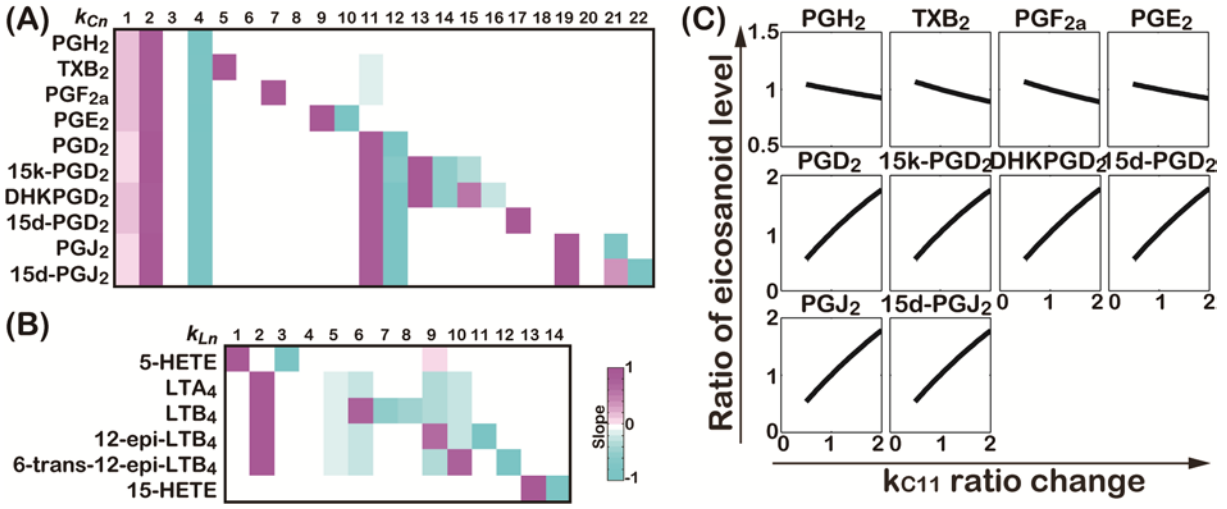


**Fig. S3 Parametric sensitivity analysis.** The slope of the sensitivity curves of COX (A) and LOX (B) pathways are shown as heat maps. The numbers represent the rate parameters $k_{Cn}$ and $k_{Ln}$. (C) The representative results of parametric sensitivity analysis for parameter $k_{C11}$ (PGH2→PGD2) are shown. The fold-changes in the maximum value of eicosanoids are plotted against the ratio change of $k_{C11}$ parameter. For example, the changes in parameter $k_{C1}/k_{C2}$ (AA→$PGH_2$) and $k_{C4}$ ($PGH_2$→) produced an increase and a decrease in all metabolites, respectively. Because $PGH_2$ was belonging to the upper part of the reaction network, the changes in these parameters produced a larger change in all metabolites. Similar results were observed for the changes in parameter $k_{L2}$ and $k_{L5}$ in LOX pathway. In our model, $PGD_2$ was one of the hubs of the reaction network. It was metabolized to 13,14-dihydro-15-keto-$PGD_2$ (DHK-$PGD_2$), 15-deoxy-$\Delta^{12,14}$-$PGD_2$ (15d-$PGD_2$) and $PGJ_2$. Therefore, all metabolites downstream of $PGD_2$ were affected to the same degree as $PGD_2$ for change in the parameter $k_{C11}$ ([*Ptgds2*]$PGH_2$→$PGD_2$).

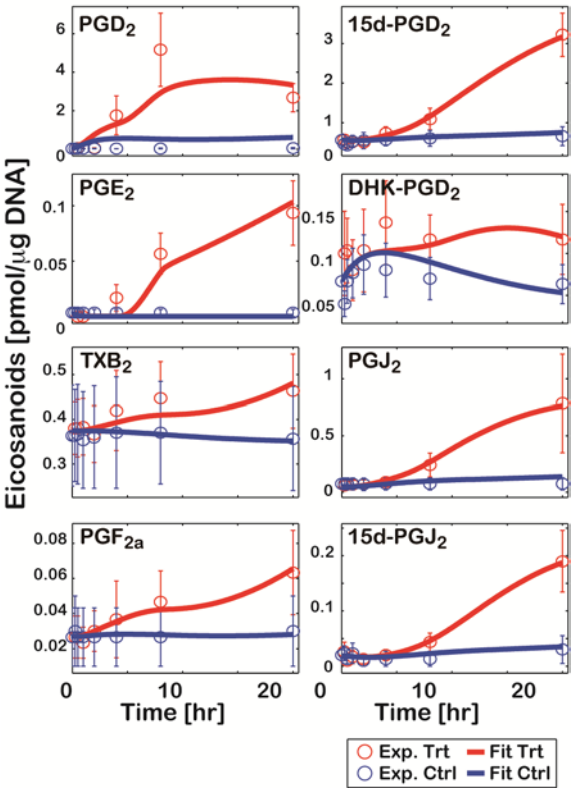


**Fig. S4 Computational simulation of eicosanoid metabolism by $PGH_2$-divided model.** The experimental data (Exp) of ATP-treated (Trt) and control (Ctrl) represent means ± SEM. The simulation results (Fit) are shown as red and blue curves for Trt and Ctrl, respectively.

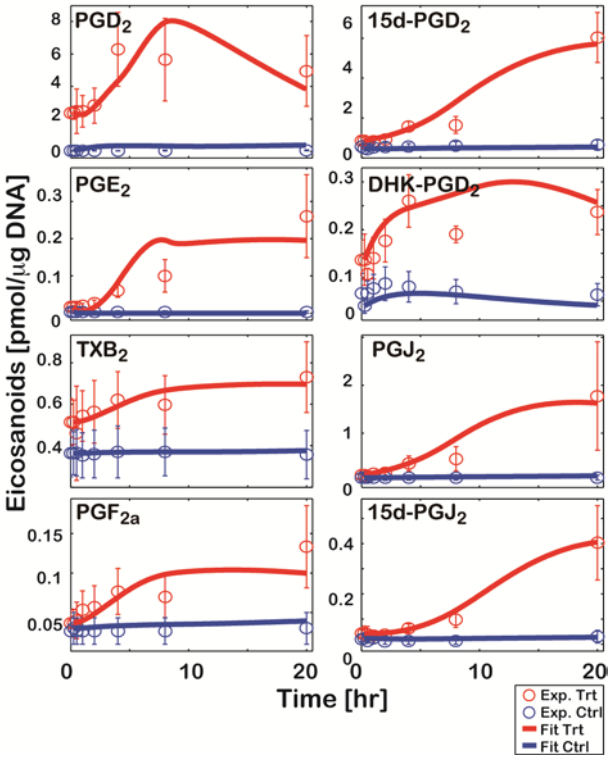


**Fig. S5 Prediction of the eicosanoid profile in KLA-primed ATP-stimulated BMDMs by $PGH_2$-divided model.** The experimental data (Exp) of KLA-primed ATP-treated (Trt) and control (Ctrl) represent means ± SEM. The simulation results (Fit) are shown as red and blue curves for Trt and Ctrl, respectively.